Geopersia ***10*** *(1), 2020, PP. 101-113* *DOI: 10.22059/GEOPE.2019.259459.648392*

The Effect of Nano-Kaolinite on Liquefaction Resistance of Liquefiable Sand

Rasool Yazarloo, Mashalah Khamehchiyan*, Mohamamd Reza Nikudel
Department of Geology, Tarbiat Modares University, Tehran, P.O. Box: 14155-111, Iran
**Corresponding author, e–mail: khamechm@modares.ac.ir*
(*received: 03/06/2018 ; accepted: 07/07/2019*)

Abstract

Nanotechnology has played a significant role in the improvement of the problematic soils. This study was to investigate the effect of the nano-kaolinite concentration on the liquefaction resistance of liquefiable sand from Gorgan, Iran. To examine the influence of the nano-kaolinite concentration on the liquefaction resistance of nano-kaolinite-sand mixtures, three different nano-kaolinite concentrations (namely 3%, 6%, and 9%) were prepared. In order to simulate the earthquake impact on the liquefiable sand, cyclic triaxial tests were conducted on pure sand and nano-kaolinite-sand mixtures. Cyclic triaxial test was repeated two times for each nano-kaolinite-sandy soil mixture and the mean and standard deviation values of total 24 tests were obtained. Based on the obtained results, nano-kaolinite concentration has a contradictory effect on the liquefaction resistance of the studied soil. It was found that the influence of nano-kaolinite concentration on liquefaction resistance of the sand should be evaluated using a critical value of nano-kaolinite concentration. Below the critical value (under 6% nano-kaolinite content), liquefaction resistance decreases as the nano-kaolinite concentration increases. Beyond such a value, liquefaction resistance enhances with an increase in nano-kaolinite concentration. The results showed that the nano-Kaolinite–sand samples with 9% nano-Kaolinite concentrations show liquefaction resistance much more than untreated soil. It was also observed that at the same cyclic stress ratio, liquefaction resistance and axial strain of samples decreases as the confining pressure increases.

Keywords: *Nano-Kaolinite; Liquefaction; Cyclic Triaxial Test; Gorgan.*

Introduction

Liquefaction, a costly geotechnical hazard, results from a rapid and dramatic strength loss of the saturated loose sands and deposits, which is caused by excess pore-water pressure imposed by dynamic loading. Liquefaction leads to the loss of soil bearing capacity and soil settlement, as well as large deformation. This in turn results in the destruction of structures such as lifeline systems, harbor facilities, and so on (Erken, 2001; Chu *et al.,* 2003; Yuan *et el.,* 2003; Ku *et al.,* 2004; Sonmez *et al.,* 2008). Several improvement methods have been developed since the 1964 Niigata earthquake, which caused serious damages to buildings due to liquefaction, in order to mitigate the liquefaction potential of the liquefiable deposits. Dynamic compaction, vibratory probe, granular piles, deep mixing, and chemical grouting can effectively enhance the liquefaction resistance of the soil (National Research Council, 1985). These techniques, however, have limited applications since they would lead to significant environmental disturbance. Previous studies have indicated that clay-sized particles (< 0.002 mm) can effectively reduce the liquefaction potential of the soil (Chang & Hong, 2008; Dimitrova & Yanful, 2012; Ku & Juang, 2012).

In recent years, nano-materials have been increasingly used to improve the primary properties of liquefiable soils in the laboratory. Nano-materials have specific features, including high surface activity and specifically broad surface area. The grain size of nanomaterials does not exceed 100 nm (Cao, 2004; Huang & Wang, 2016a). The application of nanomaterials in geotechnical engineering reflect their superiority in terms of price/performance ratio and environmental effects, in comparison to the traditional techniques (Huang & Wang, 2016a).

A number of studies have investigated the effect of various nanomaterials on different properties of soil (Majeed & Taha, 2012; Mohammadi & Niazian, 2013; Firoozi *et al.,* 2014; Changizi & Haddad, 2015; Changizi & Haddad, 2017; Huang & Wang, 2016b). Three significant mechanisms through which nonmaterials enhance the liquefaction resistance of the soil include soil grain cementation, pore fluid solidification, and delay of pore pressure response. An increase in liquefaction resistance using colloidal silica (particles size between 7 and 22 nm) has been documented in laboratory tests (Gallagher & Mitchell, 2002), model tests (Gallagher *et al.,* 2007a), and full-scale field tests (Gallagher *et al.,* 2007b).

This study aimed to investigate the effect of nano-kaolinite concentration on the mitigation of

liquefaction in liquefiable sand samples from Gorgan, Iran. The main objective of the present study was to investigate the effect of nano-kaolinite concentration on liquefaction resistance of sand using triaxial cyclic test. Moreover, the behavior of soil under different nano-kaolinite concentration was to be evaluated.

Material and methodology

Used soil

The Caspian Lowland of Northern Iran is a part of the Eurasian loess belt. This belt extends from Central Asia and China to the Northwest Europe. Dusts and loess accumulated in the northern Iran during the Pleistocene glaciations (Frechen *et al.,* 2009). Pleistocene loess transported across a short distance because these soils possess coarse dust components (Wang *et al.,* 2017). Previous studies showed that the deposits in Gorgan are prone to liquefaction (Majdi *et al.,* 2007; Mostafazadeh & Ownegh, 2012). Using geological and geomorphological maps (Fig. 1a) and available boreholes (Fig. 1b), Gorgan's sedimentary model was obtained by AutoCAD 2015 software (Fig. 1b). The results of 61 boreholes were analyzed to reach this model. The liquefiable soil (SP) was sampled from Gorgan using rotary-percussion drilling method. Worth to note that disturbed samples were taken using the SPT sampler. Soil was taken from SP unit at the depth of 18 m (Fig. 1b). The maximum depth at which liquefaction can occur is relatively identical to the maximum depth at which sands can remain unconsolidated (Stewart & Knox, 1995). The excessive pore water pressures can exist at depths above 30 m to overcome the stiffness caused by overburden pressures and to exceed the liquefaction thresholds. The results of standard penetration test showed that the N-values changes from 17 to >50. N-values higher than 50 were attributed to the presence of boulder and gravel in this unit. As shown in Fig. 1, CL soil is the main unit 25 meters below the ground surface. Also GP, ML and SP soils are available in the sampling area. Nowroozi and Ahmadi (1986) noted that an earthquake with a magnitude of 7.5 per century could occur in the northern and northeastern parts of Iran, which is one of the most seismically active areas in Iran.

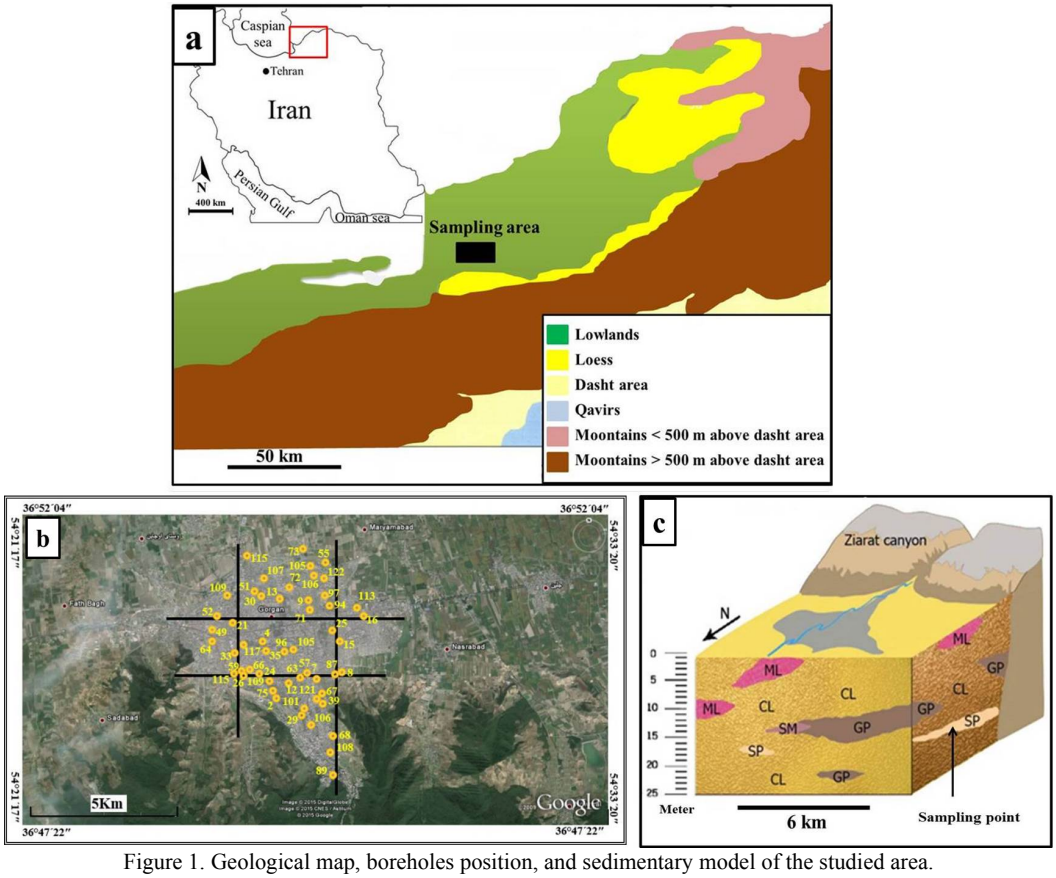

Figure 1. Geological map, boreholes position, and sedimentary model of the studied area.

Gorgan plain is located in a dry to semi-wet area. Average annual rainfall varies from 250 to 750 mm which cause in high groundwater table (Yazdani & Kowsari, 2013).

The gradation (ASTM D6913/D6913M-17), void ratio, relative density, and unit weight (ASTM D4254 -16) of the studied soil were measured in the laboratory. The results showed that the soil could be classified as poorly graded sand (SP) according to the unified soil classification system. The physical properties of soil are listed in Table1. Grain size distribution of the studied soil is illustrated in Fig. 2. The sample was studied under scanning electron microscopy (SEM) in order to determine the grain shape and the fabric of remolded soil (Fig. 3). The Sharp corners of the soil particles represent the short transportation distance.

Kaolinite

Kaolinite was sampled from the quarries of Zonouz city, located in the Eastern part of Azarbaijan province.

Table 1. Physical properties of the studied soil.

G_s	e_{min}	e_{max}	$\gamma_{d)min}$ ((KN/m^3)	$\gamma_{d)max}$ ((KN/m^3)	FC (%)	D_{50} (mm)	C_u	C_c
2.72	0.57	0.81	15.0	17.3	0	0.216	1.392	0.896

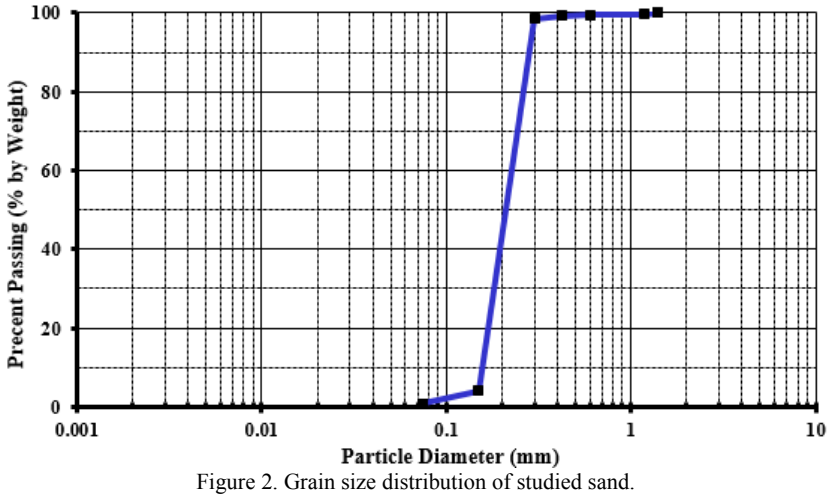

Figure 2. Grain size distribution of studied sand.

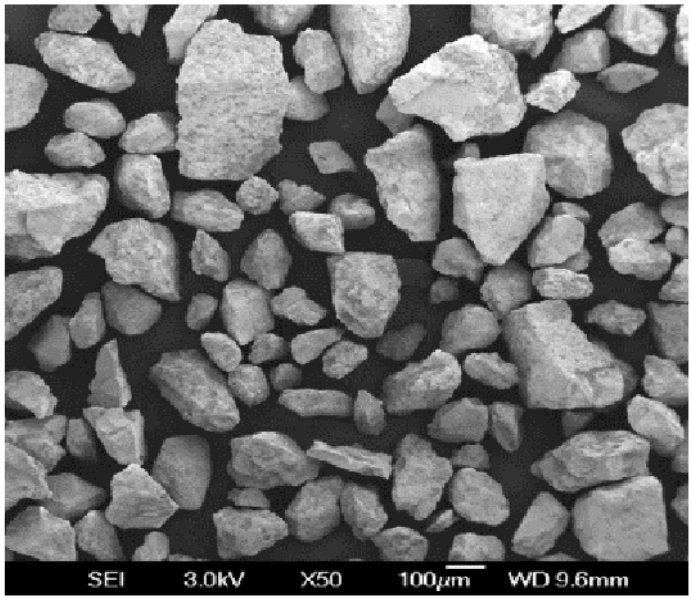

Figure 3. SEM image of the studied soil

Grain size distribution of the selected kaolinite was determined using sieve analysis and hydrometer test. The gradation test result is illustrated in Fig. 4. X-ray diffraction (XRD) and X-ray fluorescence (XRF) tests were performed to characterize the mineralogical components and elemental composition, respectively. The results of the XRD analysis are illustrated in Fig 5. AL_2O_3 and SiO_2 are two major elements of kaolinite clay (Table 2). Plasticity tests were also conducted to determine the Atterberg limit of kaolinite according to ASTM D4318-17e1 (2006). The results of plasticity tests are presented in Table 3. The mean plastic limit, liquid limit, and plastic index were found to be 31%, 69% and 38, respectively.

Table 2. XRF test

Composition	**Rb**	**Fe_2O_3**	**CaO**	**K_2O**	**SO_3**	**P_2O_5**	**SiO_2**	**Al_2O_3**	**MgO**	**L.O.I**
(%)	0.01	0.76	0.05	1.45	0.03	0.10	47.16	38.23	0.34	11.87

Table 3. Mean values of Atterberg limits and specific gravity of kaolinite

G_s	**PL (%)**	**LL (%)**	**PI**
2.72	31	69	38

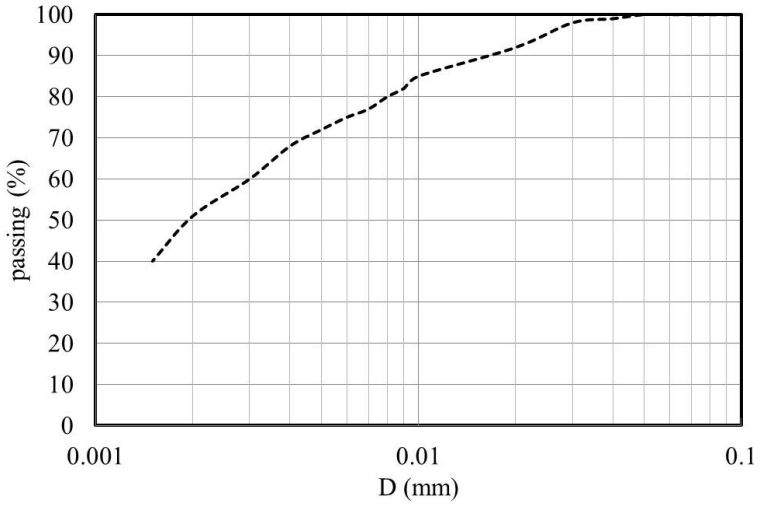

Figure 4. Grain size distribution of kaolinite.

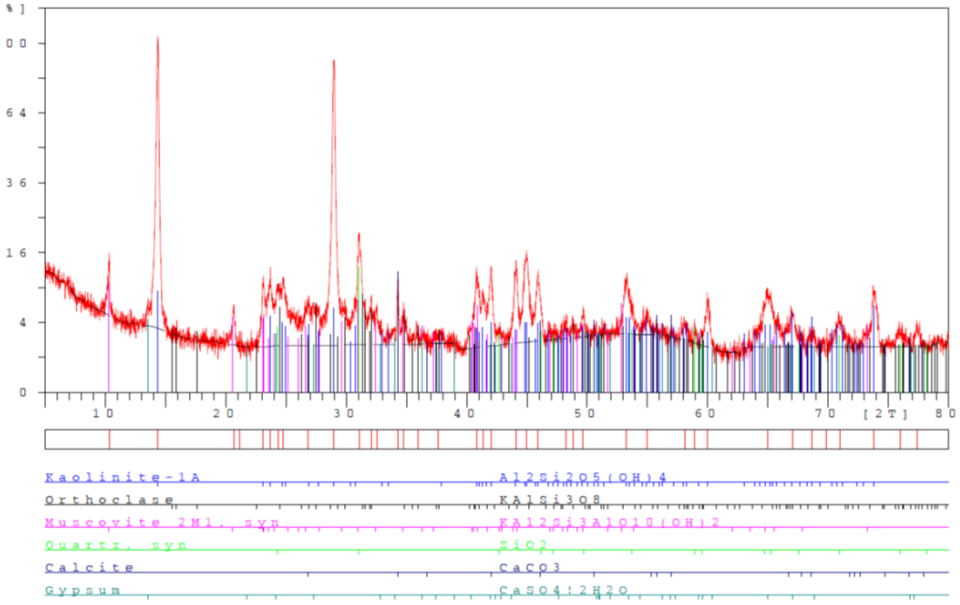

Figure 5. XRD analysis of Kaolinite.

Nano-kaolinite

Planetary ball mill was used to prepare nano-kaolinite in the laboratory. To this end, two 250-ml steel milling jars along with steel grinding balls of 10 and 15 mm diameter were used. Nano-kaolinite preparation process was performed at different milling speed and Field Emission Scanning Electron Microscope (FESEM) was applied to determine optimum milling speed, time, and ball diameter (Fig. 6). Optimum performance of planetary ball mill in producing nano-kaolinite is presented in Table 4. FESEM image was used to measure the mean nano-kaolinite particles size using JMicrovision software. The mean size of nano-kaolinite particles was estimated to be about 60 nm.

Sample preparation

Liquefaction resistance of the soil treated with nano-kaolinite was assessed through dynamic triaxial tests. To evaluate the influence of the nano-kaolinite concentration on the liquefaction resistance of nano-kaolinite-sand mixtures, three different nano-kaolinite concentrations (namely 3%, 6% and 9%) were prepared in the laboratory. Several sample preparation methods are proposed in the literature (Huang & Wang, 2016a). Dry mixing techniques are found to be the most suitable ones to prepare nano-kaolinite-sand mixtures. The dry mixing technique was selected to maximize reproducibility since the nano-particles completely fill the soil pores as they dry-mixed (Persoff *et al.,* 1999). Sand and nano-kaolinite were dry-mixed by shaking in a bottle for 5 minutes. The mixtures of sand and nano-kaolinite were transferred to the plexiglass-cylindrical container with a diameter of 50 mm. Sand and nano-kaolinite were dry-mixed by manual shaking for 20 minutes. The cylindrical container of plexiglass was then placed on the cylindrical mold with a diameter of 54mm (Fig. 7). The height of samples was 120 ±5 mm.

The sample saturation procedure consists of the following stages: 1) flushing the specimen with carbon dioxide gas (CO_2), 2) saturation with water, and 3) back pressure saturation. Samples were flushed with carbon dioxide gas at the water pore pressure maintained in 7-10 kPa for 30 minutes. Flushing helps in achieving saturation at a faster rate. Saturation of sample with CO_2 and water could lead to the immigration of fines to the bottom of sample. To deal with this problem, the pumping pressure of CO_2 and water are kept in low value (3-8 kPa). Full saturation occurs as the B-values reaches ≥0.96.

Table 4. Optimum performance of planetary ball mill in producing nano-kaolinite

Ball composition	Ball size (mm)	Milling time (h)	Spin speed (PRM)
Steel	10 (10 ball)	10	520

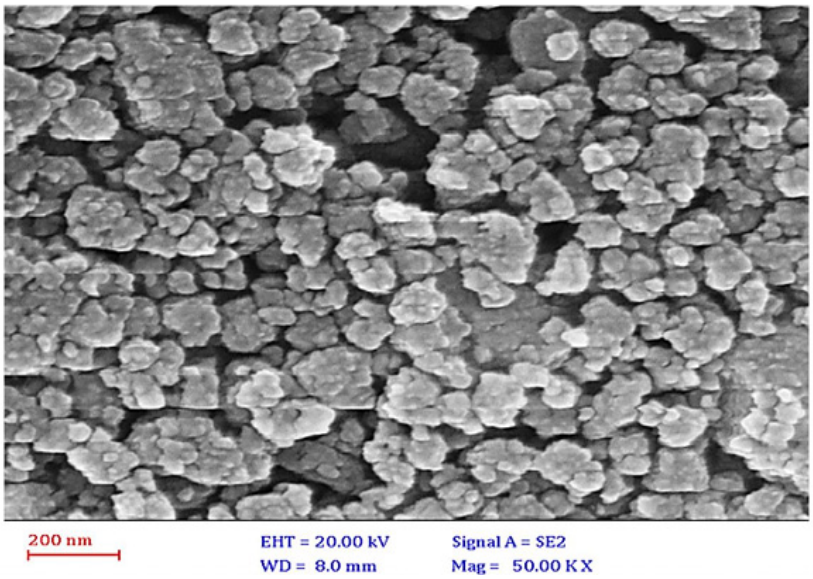

Figure 6. FESEM images of nano–kaolinite.

Relative density has a large impact on the liquefaction resistance of soils. Maximum and minimum unit weights of the prepared samples were obtained according to ASTM D4253-00 (Table 5). The samples were prepared with relative density of 45%. Firstly, the samples weighted and then compacted within the cylindrical container to achieve a similar relative density.

Triaxial cyclic test

In this study, cyclic triaxial tests (ASTM D5311-13) were carried out on the samples of liquefiable poorly-graded sand mixed with different nano-kaolinite concentrations. All experiments were performed under undrained conditions in order to simulate dynamic earthquake loading. Triaxial cyclic test is costly to perform. For each nano-kaolinite-sand mixture, two tests were run and the mean and standard deviation values of the data were obtained. A Total number of 24 triaxial cyclic tests were conducted on the samples. Small standard deviation values were recorded for two repeated tests.

Cyclic stress ratio (CSR) is one the most important parameters affecting the liquefaction resistance of the soil (Polito, 1999, Papadopoulou & Tika, 2008). It should be mentioned that all experiments were performed at the same cyclic stress ratio (CSR=0.25) and different confining stress of 100, 150 and 200 kPa. Soil consolidation has a significant impact on the liquefaction resistance. It is worth to note that all samples were consolidated at a pressure equal to test confining pressure. Applying back pressure is the final step after ensuring the sample saturation. In the present study, each sample was tested at three different confining pressures (100, 150 and 200 kPa), and the samples were consolidated under these pressures. Consolidation occurred within about 30 min for pure sand; however, the consolidation of nano-kaolinite-sand mixture took 3-4 hours or more.

Results and discussion

The mean values of triaxial cyclic tests are presented in Table 6. The results of triaxial cyclic tests for untreated sand at CSR=0.25 and confining pressure of 100 kPa are illustrated in Fig. 8. An increase in cyclic load under constant CSR led to an increase in axial strain.

Table 5. Mean values of maximum and minimum unit weights for the prepared samples.

Nano-kaolinite content (%)	e_{min}	e_{max}	γ_{min} (kN/m^3)	γ_{max} (kN/m^3)
0	0.55	0.81	14.91	17.77
3	0.47	0.79	15.26	18.71
6	0.43	0.77	15.44	19.01
9	0.44	0.79	15.32	18.91

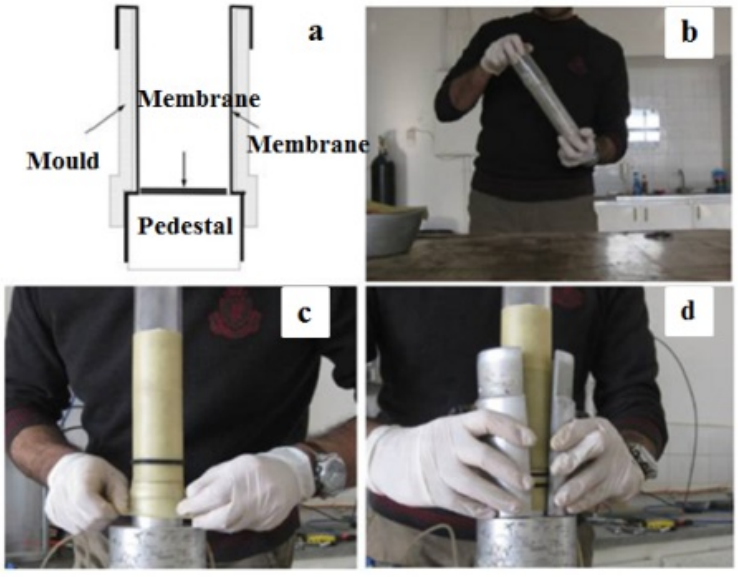

Figure 7. Sample preparation steps: a) schematic view of prepared sample, b) shaking the bottle containing nano–kaolinite–sand mixture, c) mounting the sample on pedestal, and d) placing plexiglass in cylindrical mold.

Table 6. Mean of triaxial cyclic test.

Content of Nano-kaolinite (%)	Number of test	Confining pressure (kPa)	Cyclic stress ratio (CSR)	Axial strain (%)	Excess pore pressure (kPa)	Number of cycle to liquefaction
0	2	100	0.25	5.2 ± 0.07	105.2 ± 7.02	54 ± 2.8
0	2	150	0.25	4.8 ± 0.42	156.0 ± 6.13	41 ± 4.24
0	2	200	0.25	5.1 ± 0.17	207.5 ± 9.32	37 ± 1.41
3	2	100	0.25	5.3 ± 0.14	107.1 ± 5.46	20 ± 2.82
3	2	150	0.25	5.1 ± 0.11	156.3 ± 4.78	17 ± 1.41
3	2	200	0.25	4.8 ± 0.09	210.4 ± 9.27	9 ± 0.00
6	2	100	0.25	6.1 ± 0.06	108.3 ± 3.42	37 ± 4.24
6	2	150	0.25	5.7 ± 0.08	155.0 ± 7.24	33 ± 2.8
6	2	200	0.25	5.4 ± 0.10	212.0 ± 6.87	19 ± 1.4
9	2	100	0.25	6.3 ± 0.09	110.3 ± 3.17	89 ± 5.65
9	2	150	0.25	6.1 ± 0.13	157.4 ± 9.24	67 ± 4.24
9	2	200	0.25	5.7 ± 0.16	208.6 ± 10.01	58 ± 1.41

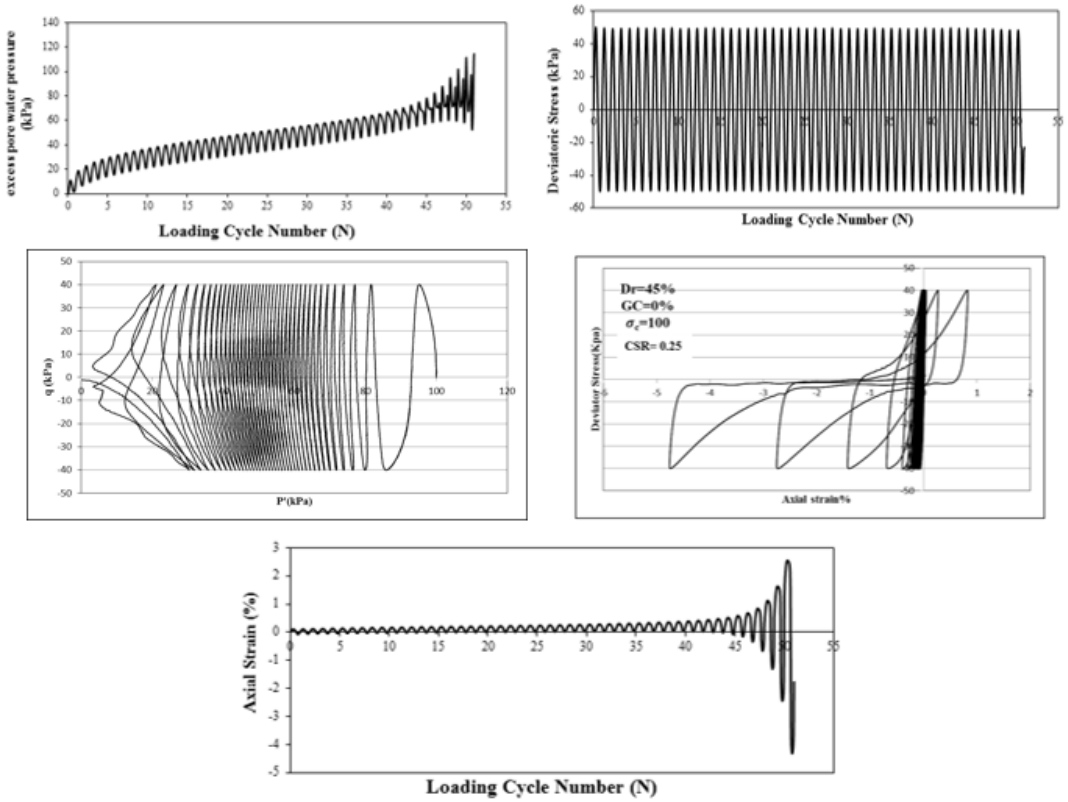

Figure 8. The results of triaxial cyclic tests for untreated soil at CSR=0.25 and confining pressure of 100kPa.

Pore pressure enhanced with increasing the number of cycles. The pore pressure of untreated sand increased to reach the confining pressure (100 kPa) in 54 loading cycles. A cyclic stress ratio of 0.25 required 54 cycles in double amplitude axial strain 5% for the untreated sand under confining pressure of 100 kPa.

As shown in Table 6 and Fig. 9, the effect of nano-kaolinite concentration on the liquefaction resistance is contradictory to some extent. Under low nano-kaolinite concentration, the liquefaction resistance decreased with an increase in the nano-kaolinite content, even though, under higher nano-kaolinite concentration, liquefaction resistance increased with an increase in the nano-kaolinite content. Consequently, the effect of the nano-kaolinite concentration on the liquefaction resistance of sand could be evaluated using a critical or threshold value of the nano-kaolinite concentration. In this study, the threshold value of

nano-kaolinite content was assessed to be 7% of the total dry mass of the sand.

Shear strength (cohesion and internal friction angle) of soil has a profound impact on the liquefaction resistance of soil. Below the critical value, the water sensitive nano-kaolinite particles seem to act as a lubricant agent for grains displacement. Consequently, the greater nano-kaolinite content results in easier grain displacement and thus higher liquefaction potential. The internal friction angle of soil is a key parameter controlling liquefaction resistance of soil. Below the critical content of the nano-kaolinite, an increase in the nano-kaolinite content leads to a decrease in the friction angel of soil and thus lower liquefaction resistance. In the nano-kaolinite-sand mixtures with high nano-kaolinite content (above the critical value), a great portion of the nano-kaolinite particles fill voids among the sand grains and act as cement. When the nano-kaolinite particles fill the gaps among the sand grains, the cohesion (the mutual connection between heterogeneous particles (nano-kaolinite and sand) increases; therefore, above the critical values, the increase of the nano-kaolinite content leads to an increased cohesion among the sand grains and nano-kaolinite particles.

A SEM micrograph of nano-kaolinite-sand mixtures 3% is illustrated in Fig. 10.

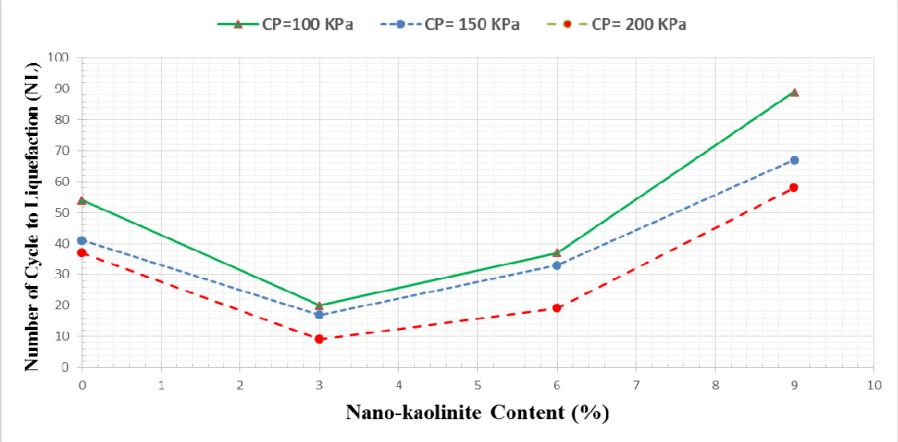

Figure 9. Liquefaction resistance of soil versus nano–Kaolinte content.

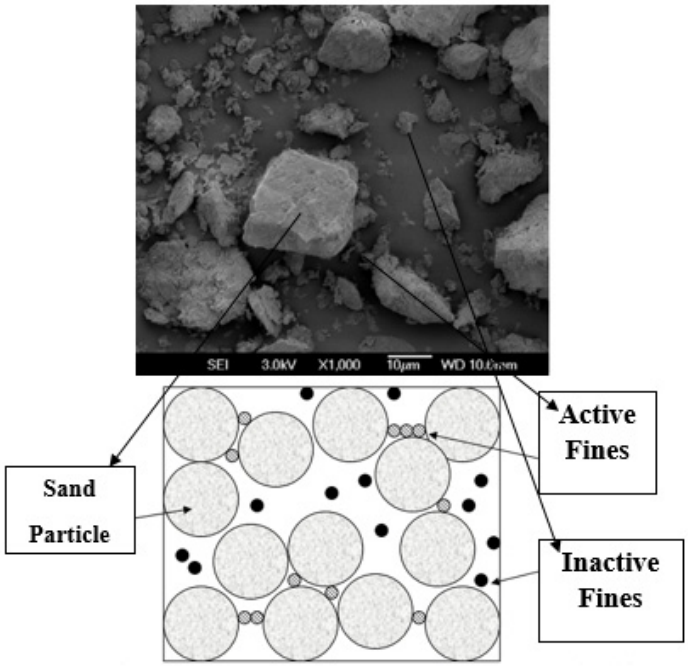

Figure 10. Microstructure of nano–kaolinite 3% (critical value) and sand sample.

Active nano-kaolinite particles are those particles acting as lubricant in the presence of water, and inactive particles fill the pores of the soil. Below the critical nano-kaolinite content, the active particles result in decreasing liquefaction resistance; however, inactive nano-particles play no significant role in liquefaction resistance. In nano-kaolinite-sand mixtures with high nano-kaolinite content (above the critical value), inactive nano-particles become active and would play an important role in mitigating the soil liquefaction. Moreover, nano-kaolinite particles can form the bridges among the larger sand grains, and consequently lead to higher liquefaction resistance. It seems that these bridges below the critical values cannot generate; however, the formation of these bridges reduces the liquefaction potential above the critical values. Marto *et al.,* (2016) examined the effect of kaolinite content on liquefaction resistance of sandy soil and found that the liquefaction resistance of soil decreases with increasing kaolinite content below the critical kaolinite content (22.5%) but above the critical value; hence, an increase in fine content resulted in enhancing liquefaction resistance. Guo and Prakash (1999) expressed that clay content can effectively increase the plasticity of liquefiable soil and liquefaction resistance. It seems that as the nano-kaolinite concentration reaches >6%, the plasticity of sandy soil increases and causes a lower liquefaction potential. Chang *et al.,* (1982) also stated that liquefaction potential of sandy soil increases when the concentration of fine grained material with low plasticity reaches 10%. They reported that liquefaction resistance of sandy soil increases as fine grained material concentration is ≥10%. Huang and Wang (2016b) mentioned that the main mechanisms through which nanoparticles mitigate liquefaction potential are pore fluid solidification, soil grain cementation, and the delay of pore pressure response.

As it can be observed in Fig. 9, the number of liquefaction cycles for soil treated with 6% nano-kaolinite at the confining pressure of 100, 150 and 200 kPa is lower than that of the untreated soil; therefore, 6% nano-kaolinite content cannot effectively enhance liquefaction resistance. The number of liquefaction cycles for the treated soil with nano-kaolinite 9% at the confining pressure of 100, 150 and 200 kPa was higher than the number of liquefaction cycles for untreated soil.

The effect of nano-kaolinite content on excess pore pressure ratio at the confining pressure of 100 kPa is illustrated in Fig. 11. Excess pore pressure has a huge impact on liquefaction-related phenomena. Excess pore pressure ratio increases with increasing the number of cycles of loads. The highest value of excess pore pressure was observed for sand treated with 9% nano-kaolinite at the confining pressure of 200kPa (Table 6). Comparison of the time series shows that nano-particles can delay the pore pressure response and limit the strain expansion so that the liquefaction potential of the treated samples decreases. Axial strain of the samples at the same CSR of 0.25 increased as the nano-kaolinite concentration enhanced (Table 6).

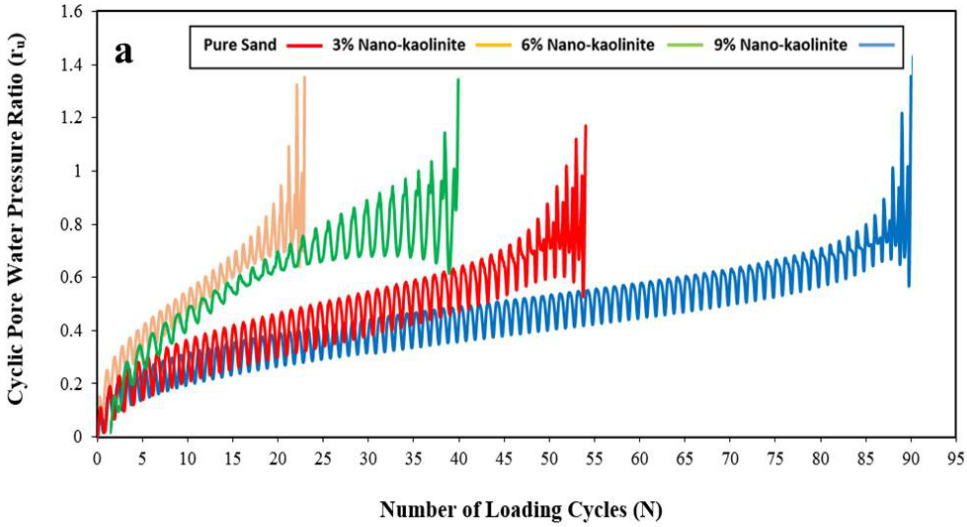

Figure 11. Excess pore pressure ratio versus the number of cycle of loads for nano–kaolinite–sand mixtures at confining pressure of 100 kPa and CSR of 0.25.

Axial strain values for the treated soil with nano-kaolinite content 3% is relatively identical to those of untreated soil; however, axial strain increases above the critical value of nano-kaolinite concentration. As it can be seen in Fig. 12, the measured number of liquefaction cycles is 54 cycles for double amplitude axial strain 5% in clean sandy soil. Increased confining pressure led to a decrease in axial strain of each mixture (Fig. 12b). The number of liquefaction cycles decreased at nano-kaolinite content 3%. The measured number of liquefaction cycles was 20 cycles in the double amplitude axial strain 5% for treated sand with nano-kaolinite 3%. The number of liquefaction cycles increased at nano-kaolinite 6% and reached 37 cycles, so the number of liquefaction cycles for treated soil with nano-kaolinite 6% was smaller than that of clean sandy soil. The number of liquefaction cycles increased at nano-kaolinite content 9% and reached 98 cycles. Our results are in line with Huang and Wang (2016b), who showed that at the same CSR, the single amplitude axial strain of the untreated sandy soil was almost 5%, twice as great as that of the nano-material–sandy soil 2% (<2%).

The effect of confining pressure on the liquefaction resistance is illustrated in Fig. 13. Confining pressure has an inverse effect on the liquefaction resistance of the soil at the constant CSR. Increasing the confining pressure leads to an increase in the axial strain at the same CSR so that the liquefaction resistance of soil decreases with an increase in confining pressure. The maximum number of liquefaction cycles was measured to be 89 cycles for treated sandy soil with nano-kaolinite content 9%. Treated sandy soil with nano-kaolinite content 3% and 6% shows lower number of liquefaction cycles than those of untreated sandy soil.

Increasing confining pressure has an inverse effect on axial strain of samples treated with the same nano-kaolinite contents (Table 6, Fig. 14).

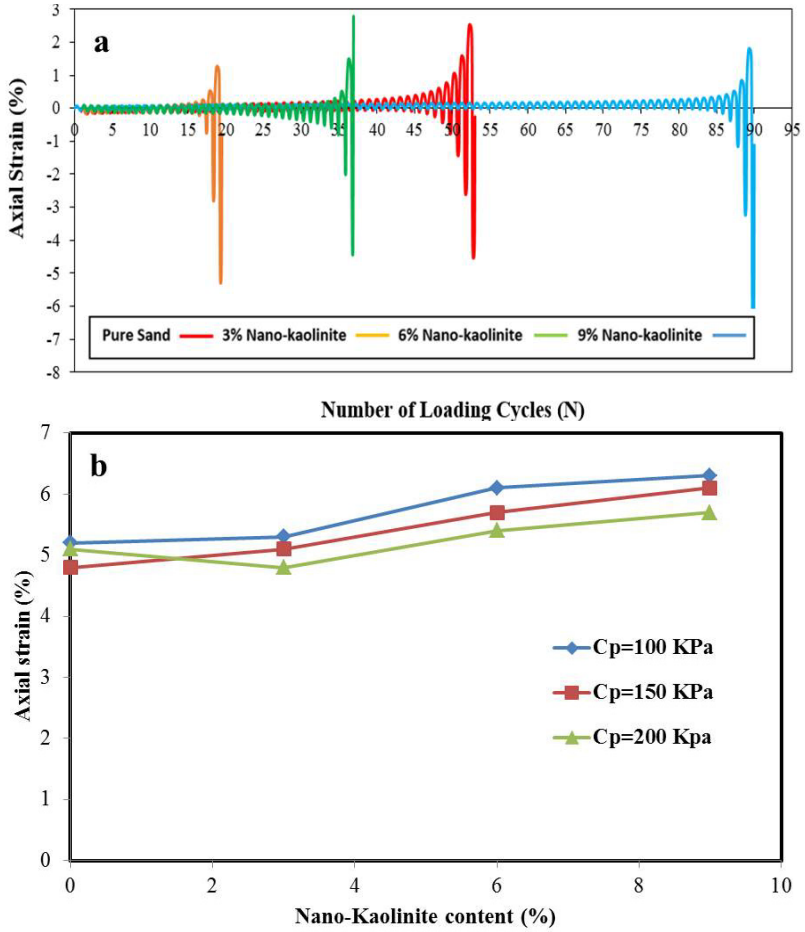

Figure 12. a) axial strain versus the number of cycle loads for liquefiable sand with nano–kaolinite content at confining pressure of 100 kPa and CSR=0.25; and b) axial strain versus nano–kaolinite content under different confining pressure.

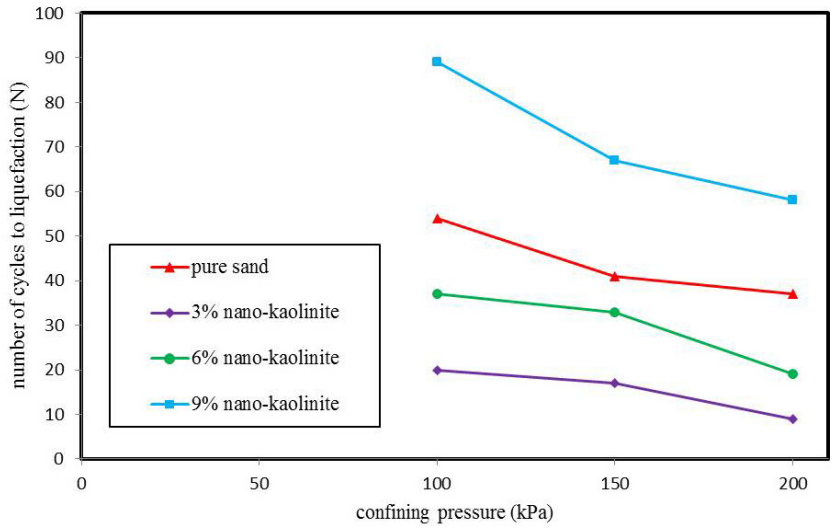

Figure 13. The effect of confining pressure on the liquefaction resistance of treated and untreated samples at the constant CSR of 0.25.

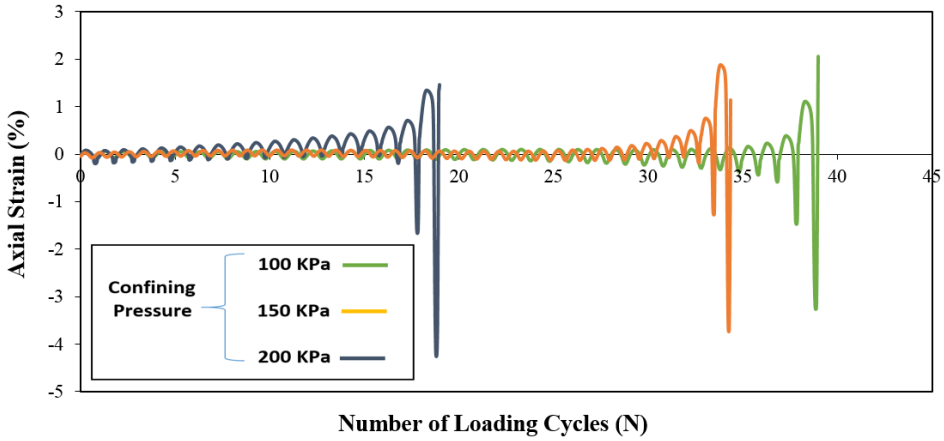

Figure 14. The effect of confining pressure on axial strain for sandy soil mixed with nano–kaolinite 6%.

Soil deformability decreases with an increase in the confining pressure. The lowest differences between axial strain at confining pressure of 100 and 200 kPa were observed for the samples treated with nano-kaolinite 9%.

Conclusion

The influence of nano-kaolinite concentration on the dynamic behavior of sandy soil was investigated using triaxial cyclic test. To examine the influence of the nano-kaolinite concentration on the liquefaction resistance of nano-kaolinite-sand mixtures, three different nano-kaolinite concentrations (namely 3%, 6% and 9%) were prepared. The major findings of this study are summarized as follows:

1: The effect of nano-kaolinite on liquefaction resistance of sand should be investigated using the critical value of nano-kaolinite content, which was found to be 7% in this study. Below the critical value, increasing the nano-kaolinite content leads to a decrease in liquefaction resistance of sandy soil. Above the critical value, liquefaction resistance increases with an increase in nano-kaolinite concentration. Below the critical value, the nano-kaolinite particles act as lubricant at saturated condition, while the nano-kaolinite particles beyond this value serve as cementation (nano-kaolinite particles fill the pores). It is worth noting that formation of nano-kaolinite bridges reduces the liquefaction potential at high nano-kaolinite contents.

2: The nano-kaolinite content to increase liquefaction resistance of Gorgan liquefiable sand was found to be >7%.

3: At the same cyclic stress ratio, the confining pressure has a negative effect on the liquefaction resistance and axial strain of sandy soils.

Acknowledgments

This study was financially supported by the Tarbiat Modares University.

References

ASTM D6913/D6913M-17, 2006. Standard Test Methods for Particle-Size Distribution (Gradation) of Soils Using Sieve Analysis. ASTM International, West Conshohocken.

ASTM D4253-00, 2006. Standard test methods for maximum index density and unit weight of soils using a vibratory table. ASTM International, West Conshohocken.

ASTM D4254-16, 2006. Standard Test Methods for Minimum Index Density and Unit Weight of Soils and Calculation of Relative Density. ASTM International, West Conshohocken.

ASTM D4318-17e1, 2006. Standard Test Methods for Liquid Limit, Plastic Limit, and Plasticity Index of Soils. ASTM International, West Conshohocken.

ASTM D5311-13, 2006. Standard Test Method for Load Controlled Cyclic Triaxial Strength of Soil. ASTM International, West Conshohocken.

Cao, G., 2004. Nanostructures and Nanomaterials-Synthesis, Properties and Applications. Imperial College Press, London, England.

Castiglia, M., Filippo, S.D.M., Napolitano, A., 2018. Stability of pipelines in liquefied soils: overview of computational methods. Geomechanics and Engineering, 14(4): 355–366

Chang, N.Y., Yeh, S.T., Kaufman, L.P., 1982. Liquefaction Potential of Clean and Silty Sands. Proceedings of the Third International Earthquake Microzonation Conference, Seattle, USA, 2:1017–1032

Chang, W.J., Hong, M.L., 2008. Effects of clay content on liquefaction characteristics of gap–graded clayey sands. Soils and Foundations, 48(1): 101–114

Changizi, F., Haddad, A., 2017. Effect of nanocomposite on the strength parameters of soil. KSCE Journal of Civil Engineering, 21(3): 676–686

Changizi, F., Haddad, A., 2015. Strength properties of soft clay treated with mixture of nano–SiO2 and recycled polyester fiber. Journal of Rock Mechanics and Geotechnical Engineering, 7(4): 367–378

Chu, B.L., Hsu, S.C., Chang, Y.M., 2003. Ground behavior and liquefaction analyses in central Taiwan–Wufeng. Engineering Geology, 71(1): 119–139

Dimitrova, R.S., Yanful, E.K., 2012. Factors affecting the shear strength of mine tailings/clay mixtures with varying clay content and clay mineralogy. Engineering Geology, 125(1): 11–25

Duman, E.S., Ikizier, S.B., Angin, Z., Demir, G., 2014. Assessment of liquefaction potential of the Erzincan, Eastern Turkey. Geomechanics and Engineering, 7(6): 589–612

Erken, A., 2001. The role of geotechnical factors on observed damage in Adapazari during 1999 earthquake. 15th ICSMGE, TC4 Satellite Conference on Lessons Learned from Recent Strong Earthquakes, Istanbul, Turkey.

Firoozi, A.A., Taha, M.R., Firoozi, A.A., Khan, T.A., 2014. Assessment of nano–zeolite on soil properties. Australian Journal of Basic and Applied Sciences, 8(19): 292–295

Frechen, M., Kehl, M., Rolf, C., Sarvati, R., Skowronek, A., 2009. Loess chronology of the Caspian low land in northern Iran. Quaternary International, 198(1): 220–233

Gallagher, P.M., Mitchell, J.K., 2002. Influence of colloidal silica grout on liquefaction potential and cyclic undrained behavior of loose sand. Soil Dynamics and Earthquake Engineering, 22(9):1017–1026

Gallagher, P.M., Conlee, C.T., Rollins, K.M., 2007a. Full–scale field testing of colloidal silica grouting for mitigation of liquefaction risk. Journal of Geotechnical and Geoenvironmental Engineering, 133(2):186–196

Gallagher, P.M., Pamuk, A., Abdoun, T., 2007b. Stabilization of liquefiable soils using colloidal silica grout. Journal of Materials in Civil Engineering, 19(1): 33–40

Guo, T., Prakash, S., 1999. Liquefaction of silts and silt–clay mixtures. Journal of Geotechnical and Geoenvironmental Engineering, Vol. 125, No. 8: 706–710

Huang, Y., Wang, L., 2016a. Experimental studies on Nanomaterials for soil improvement: a review. Environmental Earth Science, 75(6): 1–10

Huang, Y., Wang, L., 2016b. Laboratory investigation of liquefaction mitigation in silty sand using nanoparticles. Engineering Geology, 204(1): 23–32

Ku, C.S., Juang, C.H., 2012. Liquefaction and cyclic softening potential of soils—aunified piezocone penetration testing–based approach. Géotechnique, 62(5): 457–461

Ku, C.S., Lee, D.H., Wu, J.H., 2004. Evaluation of soil liquefaction in the Chi–Chi, Taiwan earthquake using CPT. Soil Dynamics and Earthquake Engineering, 24(9): 659–673

Lade, P.V., Yamamuro, J.A., Liggio, C.D., 2009. Effects of fines content on void ratio, compressibility, and static liquefaction of silty sand. Geomechanics and Engineering, 1(1): 1–15

Majdi, A., Soltani, A.S., Litkouhi, S., 2007. Mitigation of liquefaction hazard by dynamic compaction. Proceedings of

the Institution of Civil Engineers–Ground Improvement, 11(3): 137–143
Marto, A., Tan, C.S., Makhtar, A.M., Jusoh, S.N., 2016. Cyclic Behaviour of Johor Sand. International journal of GEOMATE: geotechnique, construction materials and environment, 10(21): 1891–1898.
Majeed, Z.H., Taha, M.R., 2012. Effect of nanomaterial treatment on geotechnical properties of a Penang soft soil. Journal of Asian Scientific Research 2(11): 587–592
Mohammadi, M., Niazian, M., 2013. Investigation of nano–clay effect on geotechnical properties of Rasht clay. International Journal of Advanced Scientific and Technical Research, 3(3): 37–46
Mostafazadeh, R., Ownegh, M., 2012. Assessing liquefaction hazard potential in southern Gorgan–rood plains, Golestan province. Watershed Management Research.
National Research Council (US), 1985. Liquefaction of Soils During Earthquakes. National Academy Press, Washington, the united states.
Nowroozi, A.A., Ahmadi, G., 1986. Analysis of earthquake risk in Iran based on seismotectonic provinces. Tectonophysics, 122(1–2): 89–114
Papadopoulou, A., Tika, T., 2008. The effect of fines on critical state and liquefaction resistance characteristics of non–plastic silty sands. Soils and Foundation, 48(5): 713¬–725
Persoff, P., Apps, J., Moridis, G., Whang, J.M., 1999. Effect of dilution and contaminants on sand grouted with colloidal silica. Journal of Geotechnical and Geoenvironmental Engineering, 125(6): 461–469
Polito, C.P., 1999. The effects of non–plastic and plastic fines on the liquefaction of sandy soils. Ph.D. Dissertation, Virginia Polytechnic Institute, Virginia.
Sonmez, B., Ulusay, R., Sonmez, H., 2008. A study on the identification of liquefaction induced failures on ground surface based on the data from the 1999 Kocaeli and Chi–Chi earthquakes. Engineering Geology, 97(3): 112–125
Stewart, D., Knox, R., 1995. What is the Maximum Depth Liquefaction Can Occur? Third International Conference on Recent Advances in Geotechnical Earthquake Engineering and Soil Dynamics, Volume Ill, St. Louis, Missouri.
Yazdani, A., Kowsari, M., 2013. Bayesian estimation of seismic hazards in Iran. Scientia Iranica, 20(3): 422–430
Yuan, H., Yang, SH., Andrus, R.D., Juang, H., 2003. Liquefaction–induced ground failure: a study of the Chi–Chi earthquake cases. Engineering Geology, 71(1): 141–155
Wang, X., Wei, H., Khormali, F., Taheri, M., Kehl, M., Frechen, M., Chen, F., 2017. Grain–size distribution of Pleistocene loess deposits in northern Iran and its palaeoclimatic implications. Quaternary International, 429(1): 41–51